INSTITUTE OF FLUID-FLOW MACHINERY
POLISH ACADEMY OF SCIENCES

TRANSACTIONS OF THE INSTITUTE OF FLUID-FLOW MACHINERY

112

GDAŃSK 2003

EDITORIAL AND PUBLISHING OFFICE

IFFM Publishers (Wydawnictwo IMP), Institute of Fluid Flow Machinery, Fiszera 14, 80-952 Gdańsk, Poland, Tel.: +48(58)3411271 ext. 141, Fax: +48(58)3416144, E-mail: esli@imp.gda.pl

Financial support of publication of this journal is provided by the State Committee for Scientific Research, Warsaw, Poland

Terms of subscription

Subscription order and payment should be directly sent to the Publishing Office

Warunki prenumeraty w Polsce

Wydawnictwo ukazuje się przeciętnie dwa lub trzy razy w roku. Cena numeru wynosi 20,- zł + 5,- zł koszty wysyłki. Zamówienia z określeniem okresu prenumeraty, nazwiskiem i adresem odbiorcy należy kierować bezpośrednio do Wydawcy (Wydawnictwo IMP, Instytut Maszyn Przepływowych PAN, ul. Gen. Fiszera 14, 80-952 Gdańsk). Osiągalne są również wydania poprzednie. Prenumerata jest również realizowana przez jednostki kolportażowe RUCH S.A. właściwe dla miejsca zamieszkania lub siedziby prenumeratora. W takim przypadku dostawa następuje w uzgodniony sposób.

ISSN 0079-3205

TRANSACTIONS OF THE INSTITUTE OF FLUID-FLOW MACHINERY

No. 112, 2003, 21-36

JANUSZ T. CIEŚLIŃSKI* and WALDEMAR TARGAŃSKI

Investigation of R 22 and R 134a flow boiling in enhanced tubes

Gdansk University of Technology, Narutowicza 11/12, 80-952 Gdansk, Poland

Abstract

Results of heat transfer and pressure drop investigation during flow boiling of R 22 and R 134a inside smooth tubes and selected enhanced tubes are presented. Corrugated and micro-finned tubes served as enhanced tubes. The experiments have been conducted for average saturation temperature 0°C. Inlet vapour quality was set to 0 and outlet quality: 0.7. Mass flux density varied from about 250 to 500 kg/(m^{2}s). The experimental results have been compared with heat transfer coefficients calculated from selected correlations. The test stand and experimental procedure are described. Higher average evaporation heat transfer coefficients and pressure drops for enhanced tubes have been observed. Refrigerant R 22 has an evident superiority over R 134a for each tested type of tube.

Keywords: Flow boiling; Enhanced tubes; Refrigerants

Nomenclature

a	– thermal diffusivity	F_{fl}	– fluid-dependent parameter
c	– specific heat	G	– mass flux density
d	– inside diameter	K	– parameter
h_{fg}	– latent heat of vaporisation	L	– active length of tube
k_L	– overall heat transfer coefficient for 1 m of tube length	Nu	– Nusselt number, $\mathrm{Nu}=\alpha d/\lambda$
		PF	– penalty factor, see Eq. (4)
$\dot{m}$	– mass flow rate	Pr	– Prandtl number, $\mathrm{Pr} = \eta/\alpha$
n	– exponent of Re_{lo} for augmented tubes	Re	– Reynolds number, $\mathrm{Re} = d/\mu$
		T	– temperature
q	– heat flux density	α	– heat transfer coefficient
x	– vapour quality	η	– kinematic viscosity
Bo	– boiling number, $\mathrm{Bo} = q/\dot{m}h_{fg}$	λ	– thermal conductivity

*Cornsponding author. E-mail address: jcieslin@pg.gda.pl

Co	–	convection number, $\mathrm{Co} = (\rho_v/\rho_l)^{0.5}((1-x)/x)^{0.8}$	μ	–	absolute viscosity
D	–	outside diameter	ρ	–	density
E'_{CB}	–	modified augmentation factor for convective boiling	ψ	–	heat transfer coefficient correction
E'_{NB}	–	modified augmentation factor for nucleate boiling	Φ	–	pressure drop correction
EF	–	enhancement factor, see Eq. (3)	Δp	–	pressure drop
			ΔT_m	–	logarithmic mean temperature difference

Subscripts

av	–	average	C	–	convective boiling,
l	–	liquid	N	–	nucleate boiling
lo	–	liquid only	NPB	–	nucleate pool boiling
v	–	vapour	1	–	inlet
vo	–	vapour only	2	–	outlet
w	–	water	$2F$	–	two phases

1 Introduction

In recent years, considerable efforts have been devoted to find ways to design more compact evaporators for chemical engineering and refrigeration by using enhanced heat transfer surfaces, [1-4]. These surfaces have been designed in a number of forms, from simple low integral fins to more complicated doubly enhanced tubes, [5-7].

Schlager et al. [8] studied R 22 boiling inside copper smooth and micro-finned tubes. Average saturation temperature ranged from 0 to 6°C, inlet quality from 0.1 to 0.2, outlet quality from 0.8 to 0.88 and mass flux density from 125 to 400 kg/(m^{2}s), respectively. They observed, that the heat transfer enhancement factor for the micro-finned tube was about 2.5. Eckels and Pate [9] reported the results for R 134a evaporation inside smooth and micro-finned tubes, under similar conditions. Heat transfer enhancement factor for the micro-finned tube varied from about 1.7 to 2 and the pressure drop penalty factor varied from about 1.3 to 1.7, depending on mass flux density.

International regulations, which aim at reduction of application of traditional refrigerants, have initiated searching of new working fluids. Because flow boiling is a complex process and its modelling is very difficult, experimental tests with new refrigerants are necessary [10-12].

Liu [13] compared evaporating heat transfer and pressure drop characteristics of R 134a and R 22, flowing inside copper micro-finned tube. Nominal saturation temperature was 7.2°C, inlet quality was set to 0.15 and outlet superheat ranged from 2.8 to 5.6 K. Mass flux density varied from 132.9 to 570 kg/(m^{2}s) for R 22 and from 70.5 to 393.3 kg/(m^{2}s) for R 134a. It was observed, that for mass flux density over 270 kg/(m^{2}s) the heat transfer coefficient for R 134a was lower than heat transfer coefficient for R 22 even by 50%. Pressure drop penalty factor was about 1.5.

No data for boiling in corrugated tubes have been found for R 22 as well as R 134a, although such a tube is commonly used in heat pump evaporators [14].

The aim of the study was to determine an average evaporation heat transfer coefficient and, simultaneously, pressure drop during evaporation of R 22 and R 134a inside corrugated and micro-finned tubes as well as validation of selected models for flow boiling in smooth and enhanced tubes. Smooth copper and stainless steel tubes served as reference tubes.

2 Experimental issues

2.1 Test stand

The test stand consists of four main systems: test section, refrigerant loop, heating water loop and cooling loop. The test facility is capable of determining in-tube average heat transfer coefficient and pressure drop of refrigerant over the length of a test tube. A schematic diagram of the test stand is shown in Fig. 1.

2.2 Test section

The test section consists of a tube-in-tube heat exchanger, sight-glasses and sensors for temperature and pressure measurement on the inlet and outlet of the section. The inner tube, i.e. the test tube, is a 2 m long horizontal tube with an outer diameter of about 10 mm. The tested tubes are specified in Table 1.

The water in the annulus of 2 mm gap, surrounding the test tube, flows counter to the refrigerant flow and is used to heat the refrigerant, evaporating in the inner tube.

Temperatures of the fluid streams entering and exiting the test section are measured by thermocouples accurate to ±0.3°C. The refrigerant pressure at the inlet and outlet of the section is measured by Trafag NA25.0V pressure transducers accurate to ±0.3%.

2.3 Refrigerant loop

Refrigerant is supplied to the test section at specified conditions (temperature, flow rate, quality) by the refrigerant loop. This loop contains a condenser, subcooler, pump, filter dryer, flowmeter, regulating valve and a preheater (Fig. 1).

The refrigerant exiting the test section is condensed in a copper coil, immersed

Table 1. Tested tubes

Tube description	Diameter to base of enhancement	Thickness of enhancement or fin height	Material	Other characteristics
smooth	8 mm	–	Cu	seamless
smooth	8.8 mm	–	stainless steel	seamed
corrugated	8.8 mm	$h = 0.45$ mm	stainless steel	seamed, pitch $e = 6mm$
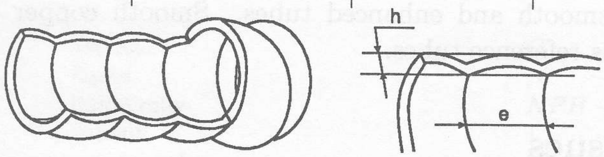				
micro-fin	8.92 mm	$h = 0.2$ mm	Cu	60 fins, seamless, twist angle $\beta = 18°C$, fin angle $\alpha = 48°C$
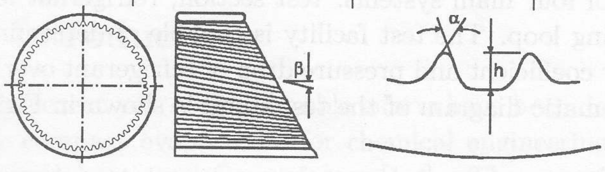				

in the 250 l glycol tank, cooled by the refrigerating unit and subcooled in the plate heat exchanger, also cooled by the refrigerating unit. The subcooled refrigerant is circulated with the pump and its flow rate is controlled with an inverter reducing the pump capacity, with the regulating valve and with a by-pass line diverting a certain portion of the flow away from the test section. Prior to entering the test section, the refrigerant temperature and quality is set in the preheater, having the form of 2.5 m long copper tube heated electrically.

Mass flow rate of ivestigated refrigerant is measured by the Danfoss MASS 2100 Coriolis-type flowmeter with accuracy of $\pm 0.15\%$ of the actual flow rate.

2.4 Heating water loop

Water is supplied to the annulus side of the test section by the water loop. This loop contains a pump, electrical heater and a flowmeter (Fig. 1). Water flow rate is controlled by a by-pass line and is measured by the magnetic flowmeter Danfoss MAG 3100 of accuracy $\pm 0.25\%$.

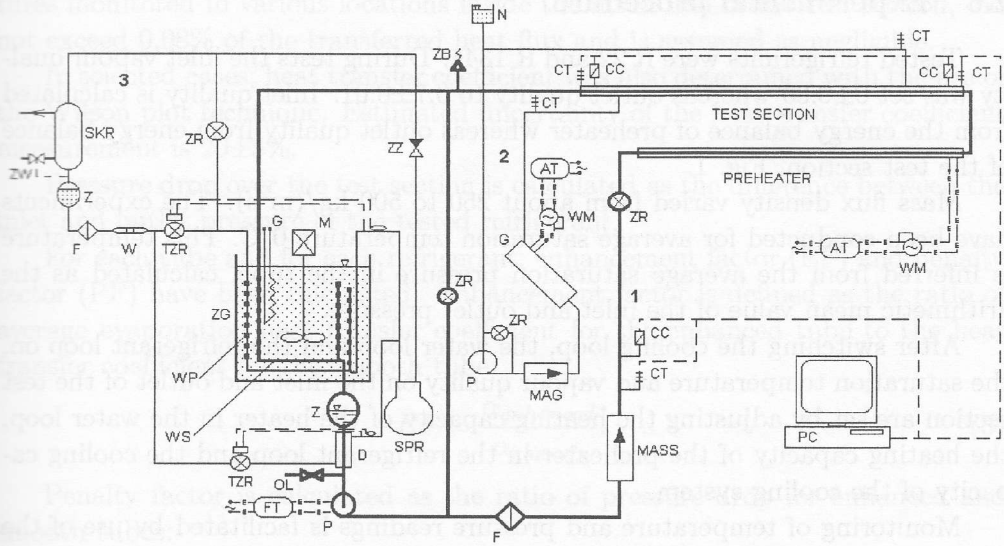

Figure 1. Test stand scheme: 1 – test loop, 2 – heating loop, 3 – cooling loop, P pump, F – filter, Z – receiver, OL – oil valve, MASS, MAG – flowmeter, ZR – regulating valve, ZB – safety valve, WS – condenser coil, WP – evaporator coil, ZG – glycol tank, M – stirrer, G – electric heater, SPR – compressor, ZZ – check valve, SKR – condenser, ZW – water regulating valve, W – sight glass, TZR – thermostatic expansion valve, N – expansion tank, D – subcooler, CC – pressure sensor, CT – temperature sensor, PC – microcomputer -aided data acquisition system, WM – wattmeter, AT – autotransformer, FT – inverter.

2.5 Cooling loop

The purpose of the cooling loop is to condense and subcool the tested refrigerant circulating in the refrigerant loop. The system contains a semi-hermetic compressor, a condenser, cooled by tap water, and two evaporators: a copper coil immersed in the glycol tank and the subcooler in the refrigerant loop (Fig. 1).

Working fluid in the cooling loop is R 22 and its flow rate in each evaporator is controlled automatically by the thermostatic expansion valve.

The maximum cooling capacity of the system is about 5 kW and the minimum recorded glycol temperature was about –30°C. It allows to keep the average saturation temperature of tested refrigerant in the test section about at –10°C. The maximum capacity of the cooling loop limits the maximum heat flux transferred to the refrigerant in the test section and is reduced by a by-pass line and three electric heaters immersed in the glycol tank, in order to obtain steady state conditions.

2.6 Experimental procedure

Tested refrigerants were R 22 and R 134a. During tests the inlet vapour quality was set 0±0.05 whereas outlet quality to 0.7±0.01. Inlet quality is calculated from the energy balance of preheater whereas outlet quality from energy balance of the test section, Fig. 1.

Mass flux density varied from about 250 to 500 kg/(m^{2}s). The experiments have been conducted for average saturation temperature 0°C. This temperature is inferred from the average saturation pressure in the tube, calculated as the arithmetic mean value of the inlet and outlet pressure.

After switching the cooling loop, the water loop and the refrigerant loop on, the saturation temperature and vapour quality on the inlet and outlet of the test section are set by adjusting the heating capacity of the heater in the water loop, the heating capacity of the preheater in the refrigerant loop and the cooling capacity of the cooling system.

Monitoring of temperature and pressure readings is facilitated by use of the PC-aided data acquisition system, Fig. 1. During each run, succesive sets of the sensor outputs were taken and processed until the readings at each power level were varied only by random amounts, so that the averages were duplicated. This was taken to be an indication, that the boiling process was at a steady state.

It takes several hours to reach the steady state after switching the test section on. After the change of parameters (for example, reduction of the tested refrigerant flow rate), the new steady state is obtained after at least 30 minutes. For each tested tube and refrigerant, the experimental points have been collected for two or three days. A good repeatability of the test results was observed.

3 Data reduction

3.1 Experimental results

In-tube heat transfer coefficient $\alpha_{2F,av}$, referred to the base surface, is calculated from the expression for overall thermal resistance:

$$\frac{1}{\alpha_{2F,av}d} = \frac{\pi}{k_L} - \frac{1}{\alpha_w D} - \frac{1}{2/\lambda}\ln\frac{D}{d}\,. \tag{1}$$

Annulus-side heat transfer coefficient α_w is calculated from the Dittus-Boelter correlation. Overall heat transfer coefficient per 1 m of tube length of the test section is:

$$k_L = \frac{c_w \dot{m}_w (T_{w1} - T_{w2})}{L\Delta T_m}\,. \tag{2}$$

The heat flux transferred to the boiling refrigerant in the test section is calculated from energy balance on the water side. Heat loss, inferred from temperatures monitored in various locations inside the insulation of the test section, did not exceed 0.08% of the transferred heat flux and is assumed as negligible.

In selected cases, heat transfer coefficient was also determined with the use of the Wilson plot technique. Estimated uncertainty of the heat transfer coefficient measurement is 20±5%.

Pressure drop over the test section is calculated as the difference between the inlet and outlet pressure of the tested refrigerant.

For each tube and for each refrigerant, enhancement factor (EF) and penalty factor (PF) have been calculated. Enhancement factor is defined as the ratio of average evaporation heat transfer coefficient for the enhanced tube to the heat transfer coefficient for the smooth tube:

$$EF = \frac{\alpha_{enhanced}}{\alpha_{smooth}}. \tag{3}$$

Penalty factor is calculated as the ratio of pressure drop for enhanced and smooth tubes:

$$PF = \frac{\Delta p_{enhanced}}{\Delta p_{smooth}}. \tag{4}$$

The ratio of these two factors EF/PF can be treated as a measure of heat transfer enhancement efficiency.

3.2 Heat transfer coefficient prediction

The experimental results have been compared with heat transfer coefficients calculated from correlations proposed by Kandlikar and Witczak [15, 16].

According to Kandlikar [15], convective and nucleate boiling heat transfer coefficients inside smooth tubes are correlated respectively:

$$\alpha_{2F,C} = 1.136\ \mathrm{Co}^{-0.9}(1-x)^{0.8}\alpha_{lo} + 667.2\ \mathrm{Bo}^{0.7}(1-x)^{0.8}F_{fl}\ \alpha_{lo}, \tag{5}$$

$$\alpha_{2F,N} = 0.6683\ \mathrm{Co}^{-0.2}(1-x)^{0.8}\alpha_{lo} + 1058\ \mathrm{Bo}^{0.7}(1-x)^{0.8}F_{fl}\ \alpha_{lo}. \tag{6}$$

For enhanced tubes Kandlikar has modified the correlations as follows:

$$\alpha_{2F,C} = 1.136\ \mathrm{Co}^{-0.9}(1-x)^{0.8}\mathrm{Re}_{lo}^{n}\ Pr_1^{0.4}E'_{CB} + 667.2\ \mathrm{Bo}^{0.7}(1-x)^{0.8}F_{fl}\ E'_{NB}, \tag{7}$$

$$\alpha_{2F,N} = 0.6683\ \mathrm{Co}^{-0.2}(1-x)^{0.8}\mathrm{Re}_{lo}^{n}\ Pr_1^{0.4}E'_{CB} + 1058\ \mathrm{Bo}^{0.7}(1-x)^{0.8}F_{fl}\ E'_{NB}, \tag{8}$$

where empirically determined constants, [15], for the micro-fin tube and R 22 are: $E'_{CB} = 82$, $E'_{NB} = 72$, $n = 0.4$.

Witczak [16] proposed correlation for convective boiling heat transfer coefficient inside smooth tubes in the form:

$$\alpha_{2F,C} = \alpha_{2F,E}(1 + \psi_{2F}), \tag{9}$$

where the equivalent coefficient:

$$\alpha_{2F.E} = \frac{1}{\frac{x}{\alpha_{vo}} + \frac{1-x}{\alpha_{lo}}}. \tag{10}$$

Heat transfer coefficient correction is defined as:

$$\psi_{2F} = 3.35x^{0.34}(1-x)^{-0.23}\Phi_{2F}^{0.34}K_{2F} \tag{11}$$

where the pressure drop correction:

$$\Phi_{2F} = 2x(1-x)\left(1-\frac{\rho_v}{\rho_l}\right)\left[\frac{(\frac{\Delta p}{\Delta L})_{vo}}{(\frac{\Delta p}{\Delta L})_{lo}} + \frac{(\frac{\Delta p}{\Delta L})_{lo}}{(\frac{\Delta p}{\Delta L})_{vo}} - 1\right]\left(\frac{\eta_l \rho_v}{\eta_v \rho_l}\right)^{0.1}. \tag{12}$$

For nucleate boiling heat transfer coefficient Witczak proposed correlation:

$$\alpha_{2F,N} = \alpha_{2F,C}\ 1.28\ K_{2F}^{0.22}(1-x)^{0.08}\left(\frac{\alpha_{2F.N}}{\alpha_{2F.C}}\right)^{0.74}. \tag{13}$$

Coefficient of heat transfer to boiling refrigerant α_{2F} is the maximum of coefficients for convective and nucleate boiling.

Correlations of Kandlikar and Witczak predict local evaporation heat transfer coefficient, i.e. for a specified boiling regime described by quality. Average values of evaporation heat transfer coefficient in the tested range of vapour quality from 0 to 0.7 were calculated as follows:

$$\alpha_{2F,av} = \frac{\int_{x1}^{x2} \alpha_{2F} dx}{x_2 - x_1}. \tag{14}$$

Equation (14) has been integrated numerically. For this purpose, the range of vapour quality is divided in 15 regions and local heat transfer coefficient was calculated for each of them, according to Kandlikar's as well as Witczak's correlations.

4 Results

4.1 Results for R 22

Experimental evaporation heat transfer coefficients for R 22 boiling inside tested tubes are plotted in Fig. 2. A linear regression analysis using the least squares method was used to determine the best-fitting straight line for what were assumed to be the steady-state results.

In the case of the micro-finned tube average heat transfer coefficients are

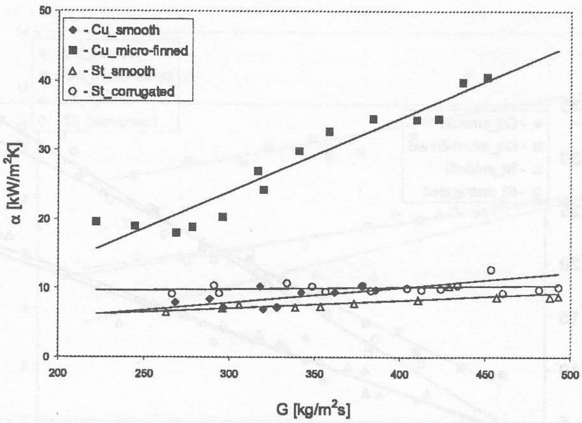

Figure 2. Average heat transfer coefficient versus mass flux density for R 22.

over two times higher, than in the smooth copper tube. Values recorded for stainless steel corrugated tube are higher, than for the smooth steel one, by over 10% in the case of the high mass flux density to under 50% for low mass flux density. Heat transfer coefficient for the corrugated tube is almost constant over the range of tested mass flux density.

Simultaneously, higher pressure drops for enhanced tubes have been recorded (Fig. 3). Pressure drop in the micro-finned tube is higher, than in the smooth copper one, by about 50% in the case of high mass flux density to about 100% for low mass flux density. In the case of stainless steel tubes, pressure drop for R 22 is higher in the corrugated tube, than in the smooth one, by over 30% for low mass flux density to over 50% for high mass flux density.

Enhancement factor and penalty factor for the copper micro-finned tube, referred to the smooth copper tube, are plotted in Fig. 4. In the case of R 22 enhancement factor increases with mass flux density increase, while the penalty factor decreases. As a result, the ratio EF/PF increases and is higher than 1 in the whole tested range of mass flux density.

For the stainless steel corrugated tube, referred to the smooth steel one enhancement factor decreases and penalty factor increases with the increase of mass flux density (Fig. 5). Only for low mass flux density, the ratio EF/PF is higher than 1.

4.2 Results for R 134a

In the case of R 134a average heat transfer coefficient during boiling in the micro-finned tube is about 50% higher, than in the case of smooth copper one (Fig. 6). Heat transfer coefficient in the corrugated stainless steel tube is higher, than in the smooth stainless steel one, by about 5% for high mass flux density to

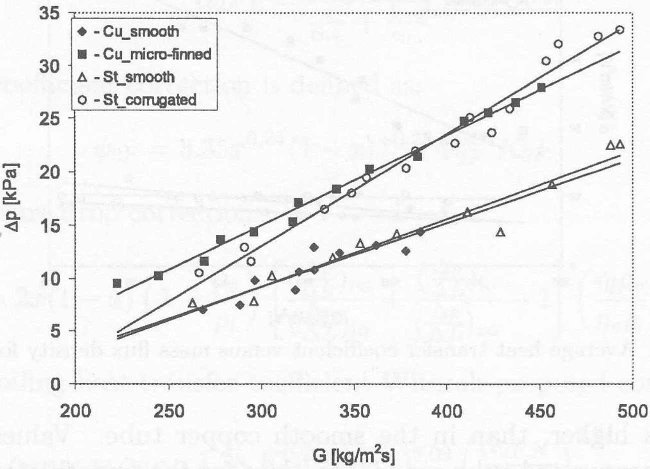

Figure 3. Pressure drop versus mass flux density for R 22.

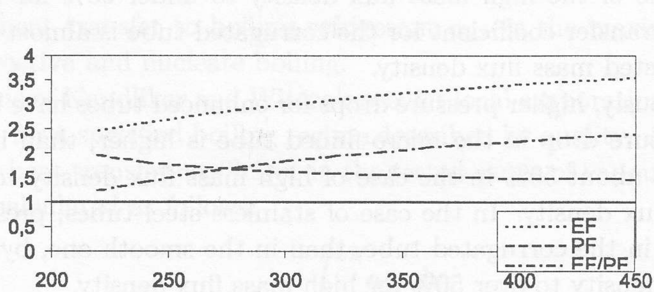

Figure 4. Enhancement and penalty factors for micro-finned tube and R 22.

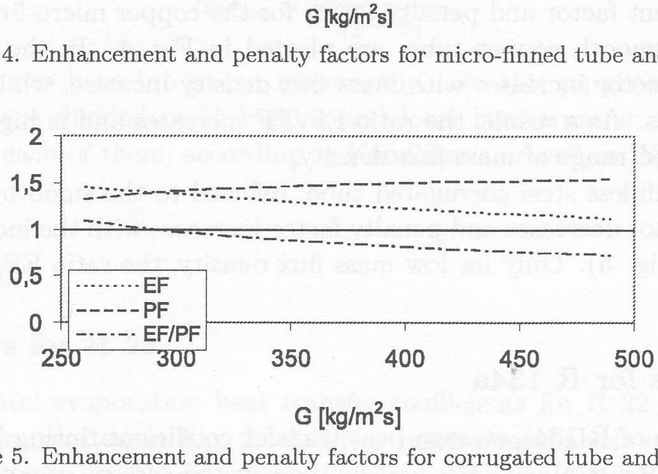

Figure 5. Enhancement and penalty factors for corrugated tube and R 22.

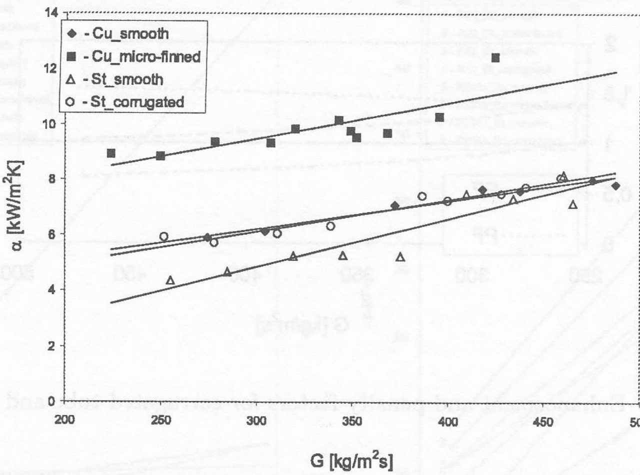

Figure 6. Average heat transfer coefficient versus mass flux density for R. 134a.

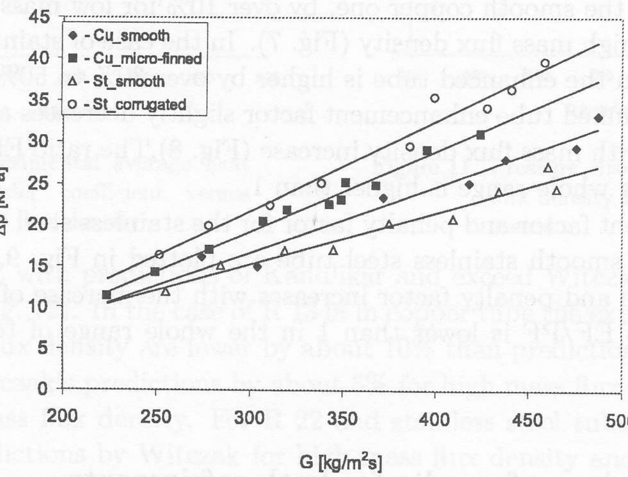

Figure 7. Pressure drop versus mass flux density for R. 134a.

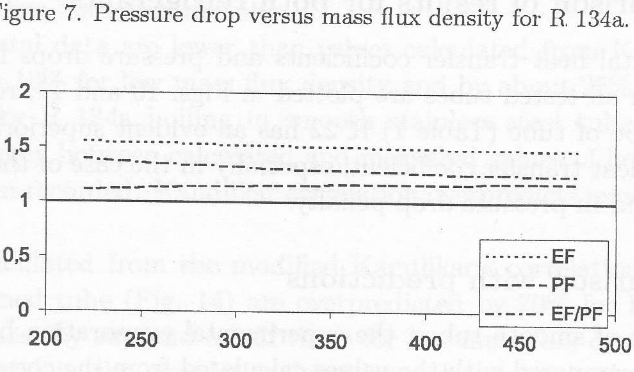

Figure 8. Enhancement and penalty factors for micro-finned tube and R. 134a.

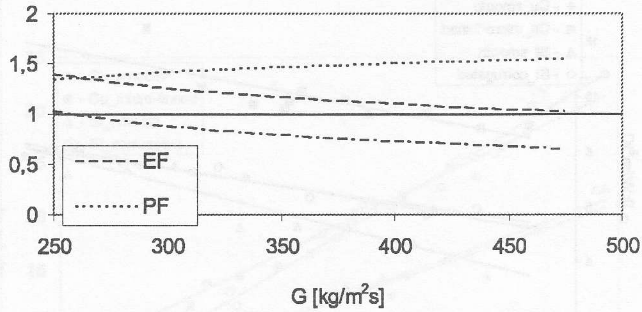

Figure 9. Enhancement and penalty factors for corrugated tube and R 134a.

about 40% for the low mass flux density.

Pressure drop during boiling of R 134a in the micro-finned copper tube is higher, than in the smooth copper one, by over 10% for low mass flux density to under 20% for high mass flux density (Fig. 7). In the case of stainless steel tubes, pressure drop in the enhanced tube is higher by over 30% to 50% respectively.

For micro-finned tube enhancement factor slightly decreases and penalty factor increases, with mass flux density increase (Fig. 8).The ratio EF/PF decreases then, but in the whole range is higher than 1.

Enhancement factor and penalty factor for the stainless steel corrugated tube referred to the smooth stainless steel tube are plotted in Fig. 9. Enhancement factor decreases and penalty factor increases with the increase of mass flux density. The ratio EF/PF is lower than 1 in the whole range of tested mass flux density.

4.3 Comparison of results for both refrigerants

Experimental heat transfer coefficients and pressure drops for R 22 and R 134a boiling in all tested tubes are plotted in Figs. 10 and 11, respectively. For each tested type of tube (Table 1) R 22 has an evident superiority over R 134a in promoting heat transfer coefficient, especially in the case of the copper micro-finned tube, and in pressure drop penalty.

4.4 Comparison with predictions

In the case of smooth tubes, the experimental evaporation heat transfer coefficients were compared with the values calculated from the correlations of Kandlikar and Witczak. For R 22 in copper tube the experimental data are in very

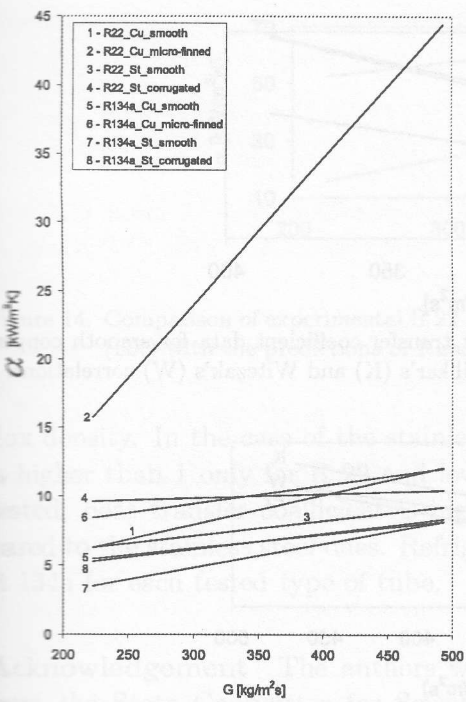

Figure 10. Experimental average heat transfer coefficient versus mass flux density.

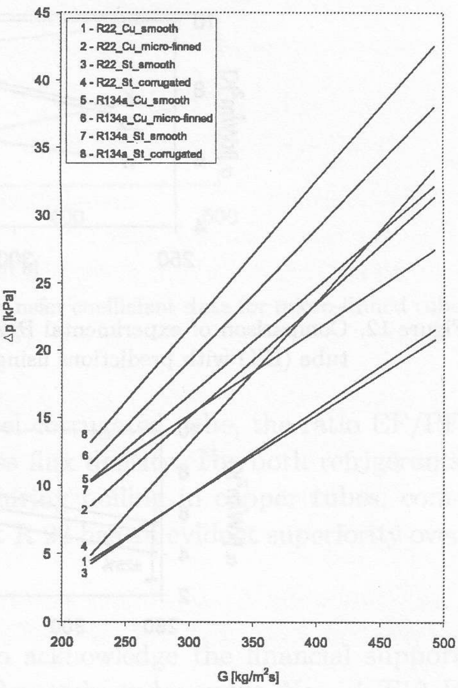

Figure 11. Pressure drop versus mass flux density for both refrigerants.

good agreement with predictions of Kandlikar and exceed Witczak's predictions by over 20% (Fig. 12). In the case of R 134a in copper tube the experimental data for high mass flux density are lower by about 10% than predictions of Kandlikar and exceed Witczak's predictions by about 5% for high mass flux density to over 10% for low mass flux density. For R 22 and stainless steel tube recorded data agree with predictions by Witczak for high mass flux density and are higher by almost 10% for low mass flux density.

Experimental data are lower than values calculated from Kandlikar's correlation by over 10% for low mass flux density and by about 25% for high mass flux density. For R 134a boiling in smooth stainless steel tube (Fig. 13) the biggest discrepancy between calculated and measured values of heat transfer coefficient has been recorded. Kandlikar correlation overpredicts experimental data by about 25%.

Values calculated from the modified Kandlikar's correlation (Eqs. 7 and 8) for micro-finned tube (Fig. 14) are overpredicted by 70% for high mass flux density and almost by two and a half times for low mass flux density. However, the constants used in the correlation have been determined experimentaly for different test conditions, i.e. higher boiling pressure and electrically heated test

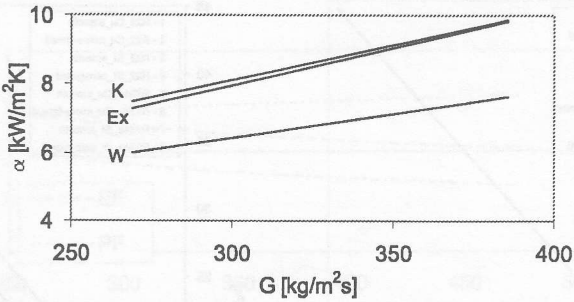

Figure 12. Comparison of experimental R 22 heat transfer coefficient data for smooth copper tube (EX) with predictions using Kandlikar's (K) and Witczak's (W) correlations.

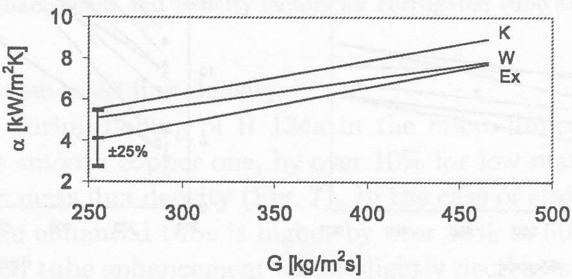

Figure 13. Comparison of experimental R 134a heat transfer coefficient data for smooth stainless steel tube (EX) with predictions of Kandlikar's (K) and Witczak's (W) correlations.

section [15].

Unfortunately, in the published literature no correlations for boiling in corrugated tubes have been found.

5 Conclusions

The results obtained for smooth tubes are in agreement with predictions obtained from correlations proposed by Kandlikar and Witczak for R 22 and R 134a as well.

For both refrigerants tested, distinctly higher average evaporation heat transfer coefficients for enhanced tubes have been observed, particularly for the micro-finned tube. Simultaneously, higher pressure drops for enhanced tubes have been recorded as well.

For the copper micro-finned tube, especially in the case of R 22, enhancement factor exceeds the area ratio, which equals 1.5. Enhancement factor decreases and simultaneously the penalty factor increases with increase of mass flux density, except the case of R 22 boiling in the copper micro-finned tube. The ratio EF/PF for the copper micro-finned tube is higher than 1 over the range of tested mass

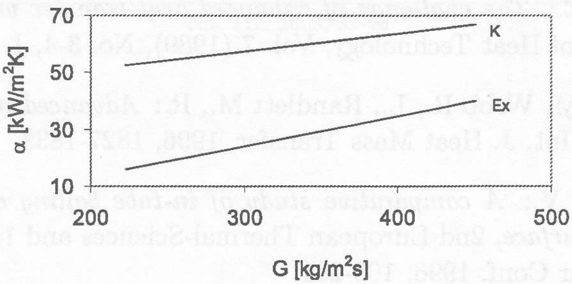

Figure 14. Comparison of experimental R 22 heat transfer coefficient data for micro-finned tube (EX) with the predictions of Kandlikar (K)

flux density. In the case of the stainless steel corrugated tube, the ratio EF/PF is higher than 1 only for R 22 and low mass flux density. For both refrigerants tested, heat transfer coefficient is higher during boiling in copper tubes, compared to the stainless steel ones. Refrigerant R 22 has an evident superiority over R 134a for each tested type of tube.

Acknowledgement The authors wish to acknowledge the financial support from the State Committee for Scientific Research under grant No. 4 T10 B 08222.

Received 20 October 2002

References

[1] Pate M., B., Ayub Z., H., Kohler J.: *Heat exchangers for the air-conditioning and refrigeration industry: State-of-the-art design and technology,* Vol. 12 (1991), No. 3, 56-70.

[2] Auracher H.: *Evaporation in tubes with special emphasis on heat transfer intensification techniques,* Proc. Eurotherm Seminar No. 3: Recent Developments in Heat Exchangers, Paris, 1993, 45-60.

[3] Thome J., R.: *Heat transfer augmentation of shell-and-tube heat exchangers for the chemical processing industry,* 2nd European Thermal-Sciences and 14th UIT National Heat Transfer Conf. 1996, 15-26.

[4] Meyer J., P.: *The performance of the refrigerants R-134a, R-290, R-404A, R-407C and R-410A in air conditioners and refrigerators,* Proc. of the ASME-ZSITS, Inter. Thermal Sci. Seminar. Bled, 2000, 67-74.

[5] Bergles A., E.: *The challenge of enhanced heat transfer with phase change,* Int. Journal of Heat Technology, Vol. 7 (1989), No. 3-4, 1-12.

[6] Chamra L., M, Webb R., L., Randlett M., R.: *Advanced micro-fin tubes for evaporation,* Int. J. Heat Mass Transfer, 1996, 1827-1838.

[7] Wadekar V., V.: *A comparative study of in-tube boiling on plain and high flux coated surface,* 2nd European Thermal-Sciences and 14th UIT National Heat Transfer Conf. 1996, 195-201.

[8] Schlager L., M., Pate M., B., Bergles A., E.: *Evaporation and condensation of refrigerant-oil mixtures in a smooth tube and a micro-fin tube,* ASHRAE Trans., Vol. 94 (1988), No. 1, 149-166.

[9] Eckels S., J., Pate M., B.: *Evaporation and condensation of HFC-134a and CFC-12 in a smooth tube and a micro-fin tube,* ASHRAE Trans., Vol 97 (1991), Part 2, 71-81.

[10] Thome J., R.: *Boiling of new refrigerants: a state-of-the-art review,* Int. J. Refrig. Vol. 19 (1996), 435-457.

[11] Kattan N., Thome J., R., Favrat D.: *Flow boiling in horizontal tubes: Part 2 - New heat transfer data for five refrigerants,* ASME J. Heat Transfer, Vol. 120 (1998), 148-155.

[12] Bohdal T., Rasmus A., Badur J.: *The investigation of bubble boiling of an environment-friendly refrigerant R 507,* Proc. of the 2 Int. Symp. on Two-Phase Flow Modelling and Exp., Rome, May 23-26, 1999. (Ed. G.P. Celata, P. di Marco, R.K Shah.) Pisa: Edizioni ETS**1999, Vol. 3, 221-224.

[13] Liu X.: *Condensing and evaporating heat transfer and pressure drop characteristics of HFC-134a and HCFC-22,* ASME J. Heat Transfer, Vol. 119 (1997), 158-163.

[14] *CETUS Heat Pumps, Product brochure of SeCesPol,* Gdańsk, Poland.

[15] Kandlikar S., G.: *A model for correlating flow boiling heat transfer in augmented tubes and compact evaporators,* ASME J. Heat Transfer, Vol. 113 (1991), 966-972.

[16] Witczak S.: *Semi-empirical model of thermo-hydraulic processes during ammonia boiling in tubes,* Studia i monografie, z. 91. Technical Univ. of Opole, 1997 (in Polish).